

# A UNIFYING MODEL OF PERFUSION AND MOTION APPLIED TO RECONSTRUCTION OF SPARSELY SAMPLED FREE-BREATHING MYOCARDIAL PERFUSION MRI

Henrik Pedersen<sup>1</sup>, Hildur Ólafsdóttir<sup>2</sup>, Rasmus Larsen<sup>2</sup>, Henrik B.W. Larsson<sup>1</sup>

<sup>1</sup>Functional Imaging Unit, Glostrup Hospital, Denmark.

<sup>2</sup>Department of Informatics and Mathematical Modelling, DTU, Lyngby, Denmark.

## ABSTRACT

The clinical potential of dynamic contrast-enhanced magnetic resonance imaging (DCE-MRI) is currently limited by respiratory induced motion of the heart. This paper presents a unifying model of perfusion and motion in which respiratory motion becomes an integral part of myocardial perfusion quantification. Hence, the need for tedious manual motion correction prior to perfusion quantification is avoided. In addition, we demonstrate that the proposed framework facilitates the process of reconstructing DCE-MRI from sparsely sampled data in the presence of respiratory motion. The paper focuses primarily on the underlying theory of the proposed framework, but shows in vivo results of respiratory motion correction and simulation results of reconstructing sparsely sampled data.

**Index Terms**— Dynamic MRI, myocardial perfusion, motion registration, sparse sampling, image reconstruction

## 1. INTRODUCTION

Within the last decade dynamic contrast-enhanced magnetic resonance imaging (DCE-MRI) has emerged as an attractive alternative to nuclear medicine techniques for the assessment of myocardial perfusion [1;2]. The method measures the delivery of the contrast agent to the myocardium during the first pass following a bolus injection, which in turn allows assessment of regional myocardial perfusion. The most immediate advantage of MRI over nuclear medicine techniques is that it does not involve any ionizing radiation and consequently carries very low risk for the patient. Also, DCE-MRI provides sufficient spatial resolution (in the order of 2-3 mm in-plane resolution) to detect subendocardial perfusion defects, and a temporal resolution of 3-4 slices per heart beat permits the use of tracer kinetic models for quantifying myocardial perfusion.

Despite these obvious advantages, DCE-MRI of myocardial perfusion has not gained wide acceptance in the clinical setting. This is partly due to a current lack of methodological consensus, but the primary bottleneck is the respiratory movement of the heart, which hampers perfusion quantification and prevents the use of modern imaging

speed-up techniques, such as k-t BLAST [3]. The accuracy of perfusion measurements is significantly improved by manual or semi-automated motion correction, but this strategy only works if the image data are fully sampled. When the data are sparsely sampled (e.g., in order to increase spatial resolution or slice coverage) respiratory motion causes severe blurring and aliasing artifacts in the subsequent image reconstruction, rendering quantification of myocardial perfusion impossible.

To the best of our knowledge, no previous work has considered respiratory motion correction, perfusion quantification, and image reconstruction as a single unified computational problem. Here we show that all three problems can be described in terms of the same unifying model equation. With this model the problem of reducing respiratory motion artifacts in DCE-MRI is considerably simplified. In the following, we first derive a general and a parameterized version of the unifying model based on tracer kinetics and optical flow theory. Next, we show how to solve and use the parameterized model in image reconstruction from sparsely sampled data. Finally, we present an in vivo example of respiratory motion correction, as well as a simulation example of reconstructing sparsely sampled data acquired during free breathing.

## 2. METHODS

### 2.1. Tracer kinetic model

The tracer kinetic models used for DCE-MRI are based on the so-called central volume principle [1]. For sufficiently low concentrations, the change in MR signal intensity (SI) is linearly related to the concentration. In this case, the tissue SI (called the *tissue residue*) is given by

$$s(t) = s_0 + F s_a(t - t_d) \otimes R(t), \quad (1)$$

where  $s_0$  is the baseline SI of the tissue before contrast arrival, and  $s_a(t)$  is the baseline-corrected SI of the arterial input function (AIF), which is typically measured in the left ventricular cavity. The operator  $\otimes$  denotes convolution,  $R(t)$  is the tissue impulse response stating the probability that a contrast molecule is still present in the voxel at time  $t$ , and  $F$

represents relative perfusion. The bolus arrival time  $t_d$  is the time it takes for the contrast agent to travel from the location where the AIF is measured to the voxel of interest.

## 2.2. Optical flow

To describe the effect of respiratory motion or motion in general, consider an image series with signal intensity  $I(\mathbf{x}, t)$ , where  $\mathbf{x} = (x, y)$  denotes a spatial position and  $t$  denotes time. Then the total derivative of  $I(\mathbf{x}, t)$  with respect to  $t$ , not to be confused with the partial derivative, is given by

$$\begin{aligned} \frac{dI(\mathbf{x}, t)}{dt} &= \frac{\partial I(\mathbf{x}, t)}{\partial x} \frac{dx}{dt} + \frac{\partial I(\mathbf{x}, t)}{\partial y} \frac{dy}{dt} + \frac{\partial I(\mathbf{x}, t)}{\partial t} \\ &= \nabla I(\mathbf{x}, t) \cdot \mathbf{u}(\mathbf{x}, t) + I_t(\mathbf{x}, t) \end{aligned} \quad (2)$$

where  $\nabla I(\mathbf{x}, t)$  denotes the gradient of  $I(\mathbf{x}, t)$ , and  $I_t(\mathbf{x}, t)$  is the partial derivative along  $t$ . The term  $\mathbf{u}(\mathbf{x}, t) = (dx/dt, dy/dt)$  is the spatial pixel velocity or optical flow field. Because  $\nabla I(\mathbf{x}, t)$  and  $I_t(\mathbf{x}, t)$  can be derived directly from the images, the unknowns of the above equation are the two components of the optical flow. We can freely choose  $dt = 1$ , such that  $\mathbf{u}(\mathbf{x}, t) = (dx, dy)$  corresponds to spatial displacement of the corresponding pixel. Equation (2) is only valid for small displacements, hence standard optical flow methods usually solve for  $\mathbf{u}(\mathbf{x}, t)$  in a coarse-to-fine manner, starting with low-resolution copies of the images and moving progressively towards the true resolution.

## 2.3. General unifying equation of motion and perfusion

If the total temporal derivative is assumed constant, one obtains the so-called *constant brightness assumption*, which forms the basis of optical flow theory. In our case, however, the total temporal derivative corresponds to the temporal derivative of the tissue residue  $s(t)$ . That is,

$$f(\mathbf{x}, t) \equiv \frac{ds(\mathbf{x}, t)}{dt} = \frac{dI(\mathbf{x}, t)}{dt}, \quad (3)$$

where we have introduced a spatial dependency on the residue. Inserting equation (2) into equation (3) yields the general unifying equation of perfusion and motion:

$$f(\mathbf{x}, t) = \nabla I(\mathbf{x}, t) \cdot \mathbf{u}(\mathbf{x}, t) + I_t(\mathbf{x}, t). \quad (4)$$

This general equation is highly underdetermined (i.e., there are more unknowns than equations). For example, if the image series consists of  $L$  pixels and  $N$  time frames, we have to solve a total of  $N \times L$  equations similar to equation (4). However, since there are twice as many unknown motion parameters (plus additional perfusion parameters), further constraints are required.

## 2.4. Unifying equation with model parameterization

In order to constrain equation (4), we assume that the tissue residue and displacement field can be parameterized (see example below) such that

$$f(\mathbf{x}, t, \mathbf{a}) = \nabla I(\mathbf{x}, t) \cdot \mathbf{u}(\mathbf{x}, t, \mathbf{b}) + I_t(\mathbf{x}, t), \quad (5)$$

where  $\mathbf{a}$  holds the parameters of the tissue residue, and  $\mathbf{b}$  represents the parameters of the displacement field. Without loss of generality, we choose a parameterization  $\mathbf{a}$  such that

$$s(\mathbf{x}, t, \mathbf{a} = \mathbf{0}) = I(\mathbf{x}, 0). \quad (6)$$

Now, assuming that the tissue residue is smoothly varying as a function of  $\mathbf{a}$ , we can approximate it locally with a first-order Taylor expansion. Accordingly, if we define  $\mathbf{a} = [a_1, a_2, \dots, a_Q]$  and expand about  $\mathbf{a} = \mathbf{0}$ :

$$s(\mathbf{x}, t, \mathbf{a}) = I(\mathbf{x}, 0) + \sum_{k=1}^Q a_k \frac{\partial s}{\partial a_k}. \quad (7)$$

Taking the temporal derivative of this expression yields

$$f(\mathbf{x}, t, \mathbf{a}) = \frac{d}{dt} s(\mathbf{x}, t, \mathbf{a}) = \sum_{k=1}^Q a_k \frac{d}{dt} \frac{\partial s}{\partial a_k}. \quad (8)$$

Since  $s$  is now analytic in  $\mathbf{a}$ , we can change the order of differentiation to obtain

$$f(\mathbf{x}, t, \mathbf{a}) = \sum_{k=1}^Q a_k \frac{\partial f(\mathbf{x}, t, \mathbf{a})}{\partial a_k} = (\nabla_{\mathbf{a}} f) \cdot \mathbf{a}. \quad (9)$$

That is, the temporal derivative  $f$  of the tissue residue can be expressed as a linear combination of  $\mathbf{a}$  and a vector containing the partial derivatives of  $f$  with respect to the parameters  $a_k$ . Inserting equation (9) into equation (5) yields the parameterized equation of perfusion and motion:

$$(\nabla_{\mathbf{a}} f) \cdot \mathbf{a} = \nabla I(\mathbf{x}, t) \cdot \mathbf{u}(\mathbf{x}, t, \mathbf{b}) + I_t(\mathbf{x}, t). \quad (10)$$

## 2.5. Example of model parameterization

Since respiratory induced motion of the heart correlates approximately linearly with the depth of respiration [4], we can parameterize the displacement by

$$\mathbf{u}(\mathbf{x}, t, b) = \mathbf{G}(\mathbf{x})b(t), \quad (11)$$

where  $\mathbf{G}(\mathbf{x})$  is a 2D displacement field (called a motion template) describing the relative orientation and amplitude

of respiratory motion between voxels, and  $b(t)$  is the respiration depth at time  $t$ . This model simplification can be extended with more motion templates to also include, e.g., hysteretic effects of respiration. In practice,  $\mathbf{G}(\mathbf{x})$  can be estimated by co-registering two images acquired in end-inspiration and end-expiration.

The tissue residue can be simplified by constraining the shape of the tissue impulse response  $R(t)$ . For instance,

$$R(t) = e^{-t/MTT} \quad (12)$$

is commonly used, where  $MTT$  denotes the mean transit time of the tracer through the voxel of interest. The AIF,  $s_a(t)$ , can be sampled in a separate (fully sampled) image series, either using a dual-bolus approach or interleaved with the tissue residue during a single bolus. We assume in the following that the AIF is sampled using one of these two approaches. Finally, we note that the baseline  $s_0$  of equation (1) simply corresponds to the SI of the initial image frame,  $I(\mathbf{x},0)$ . Thus, we get the following parameterization of the tissue residue:

$$s(\mathbf{x},t, s_a(t), I(\mathbf{x},0), \mathbf{a}) = I(\mathbf{x},0) + F(\mathbf{x}) s_a(t - t_d(\mathbf{x})) \otimes e^{-t/MTT(\mathbf{x})} \quad (13)$$

where  $\mathbf{a}(\mathbf{x}) = [F(\mathbf{x}), t_d(\mathbf{x}), MTT(\mathbf{x})]$ . The temporal derivative  $f$  and its partial derivatives with respect to  $\mathbf{a}$  can be calculated analytically using basic calculus [5]. Notice that equation (13) satisfies the condition stated in equation (7). Also notice that with the above parameterizations, we have  $3 \times L$  unknown perfusion parameters ( $\mathbf{a}$ ) and  $N$  unknown motion parameters ( $\mathbf{b}$ ). Thus, since  $L \times N \gg (3 \times L + N)$  the parameterized model equation is highly overdetermined.

## 2.6. Model fitting in the context of image reconstruction

The model parameters can be estimated using an iterative gradient-descend optimization strategy that minimizes the following cost function:

$$C(\mathbf{p}) = \left\| (\nabla_a f) \cdot \mathbf{a} - \nabla I(\mathbf{x}, t) \cdot \mathbf{u}(\mathbf{x}, t, \mathbf{b}) - I_t(\mathbf{x}, t) \right\|^2, \quad (14)$$

where  $\mathbf{p} = [\mathbf{a}, \mathbf{b}]$ . Given an estimate of the parameters  $\mathbf{p}^n$  at iteration  $n$ , we obtain

$$\mathbf{p}^{n+1} = \mathbf{p}^n - \lambda \frac{\partial C}{\partial \mathbf{p}}, \quad (15)$$

where  $\lambda$  is the update rate. As a starting guess, we can assume that there is no motion ( $\mathbf{b} = \mathbf{0}$ ) and fit the perfusion parameters ( $\mathbf{a}$ ) to the image data using a standard approach, such as the Levenberg-Marquardt algorithm.

In practice, calculating the gradient  $\partial C / \partial \mathbf{p}$  is not as computationally expensive as it may initially seem. Firstly, the partial derivatives of  $C$  with respect to  $F$ ,  $t_d$ , and  $MTT$  can be calculated separately on a per-voxel basis. That is,  $\partial C(\mathbf{x}_1) / \partial F(\mathbf{x}_1)$  is independent of  $\partial C(\mathbf{x}_2) / \partial F(\mathbf{x}_2)$  for any pair of points  $\mathbf{x}_1$  and  $\mathbf{x}_2$ , and similarly for  $t_d$  and  $MTT$ . Similarly, the partial derivative of  $C$  with respect to  $\mathbf{b}$  can be calculated on a per-frame basis, because  $\partial C(t_1) / \partial \mathbf{b}(t_1)$  is independent of  $\partial C(t_2) / \partial \mathbf{b}(t_2)$  for any pair of frames  $t_1$  and  $t_2$ .

Finally, we note that in the case of sparsely sampled MRI data, the optimal (in a least-squares sense) reconstructed image series must also minimize

$$C_{recon}(I) = \| \mathbf{WFI} - \mathbf{d} \|^2, \quad (16)$$

where  $\mathbf{d}$  represents the sampled k-space data,  $F$  is the Fourier transform, and  $W$  is a sampling function that zeros out data points in k-space that were not acquired during the sparse sampling. In order to minimize both  $C$  and  $C_{recon}$ , we propose using a fixed-point method. First, an initial estimate  $I^0$  of the image series is obtained using a conventional image reconstruction technique, such as k-t BLAST. Next, an initial guess of the perfusion parameters ( $\mathbf{a}^0$ ) is obtained using the Levenberg-Marquardt algorithm with  $I^0$  as input, and the motion parameters set to zero ( $\mathbf{b}^0 = \mathbf{0}$ ).

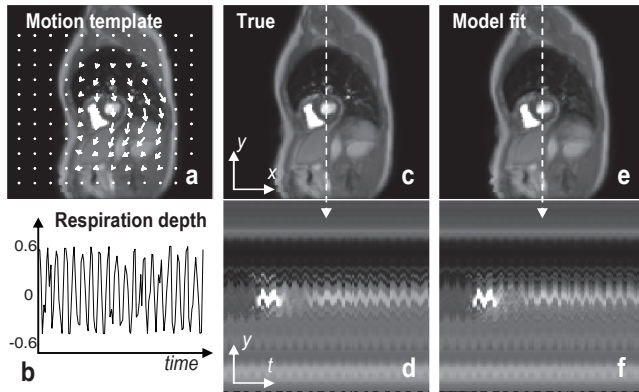
For the  $(n+1)$ 'th iteration, we denote the model parameters of the previous iteration  $\mathbf{a}^n$  and  $\mathbf{b}^n$ , and the corresponding modelled image series is denoted  $I_{\mathbf{p}}^n$ . Then we update the image series using the gradient descend rule

$$I^{n+1} = I_{\mathbf{p}}^n - \lambda \left( 2F^{-1}(\mathbf{WFI}_{\mathbf{p}}^n - \mathbf{d}) \right), \quad (17)$$

where  $F^{-1}$  is the inverse Fourier transform. The model parameters are then updated according to equation (15) using  $I^{n+1}$  as input, thereby obtaining new model parameter estimates  $\mathbf{a}^{n+1}$  and  $\mathbf{b}^{n+1}$ .

## 3. RESULTS

Figure 1 shows the results of fitting the proposed model to fully sampled in vivo data set acquired during free breathing. The estimated motion template  $\mathbf{G}(\mathbf{x})$  and respiration depth  $b(t)$  are shown in Figure 1(a-b). The perfusion parameter maps are not shown explicitly. Instead, the image frame at maximum contrast enhancement is shown, along with a time profile aligned through the left ventricle. The slow temporal changes of the time profile correspond to the contrast bolus passage, while the rapid temporal changes reflect respiratory motion. In this example, the modelled data shown in Figure 1(e-f) matched the true data in Figure 1(c-d) reasonably well.



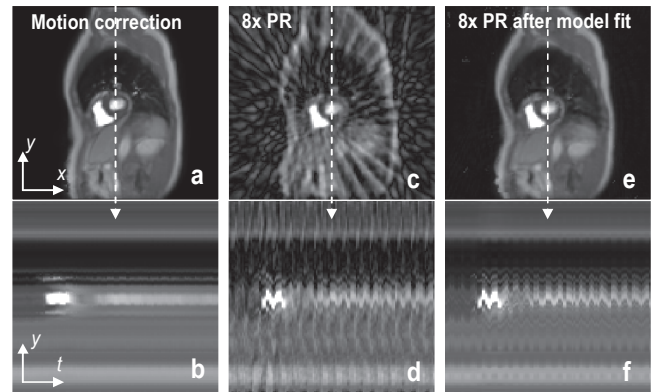
**Figure 1** - Example model fit using fully sampled in vivo data: (a) estimated motion template  $\mathbf{G}(\mathbf{x})$ , (b) estimated respiration depth  $b(t)$ , (c) true image frame at maximum contrast enhancement, (d) true time profile through the left ventricle, (e) fitted image frame, and (f) fitted time profile.

Figure 2 shows examples of respiratory motion correction and image reconstruction from sparsely sampled data using the proposed unifying model of perfusion and motion. As shown in Figure 2(a-b), the model fit achieved a near perfect correction of respiratory motion (compare with images before motion correction in Figure 1). The sparsely sampled data were radial sampled from the true data shown in Figure 1 with a sampling percentage of 12.5% (i.e., 8x data reduction). The conventional projection reconstruction (PR) in Figure 2(c-d) showed the conventional streaking artifacts caused by signal aliasing. By contrast, the proposed scheme for reconstruction of sparsely sampled data resulted in more reliable reconstruction with almost no visible streaking artifacts, as shown in Figure 2(e-f)

#### 4. CONCLUSIONS

We have presented the theory and experimental verification of a unifying computational model that simultaneously describes perfusion and motion in DCE-MRI. The method has been presented in the context of myocardial perfusion imaging, but it applies to perfusion imaging in other organs (e.g., kidneys and liver) as well. Our preliminary results suggest that the proposed model can reduce respiratory motion artifacts in myocardial perfusion DCE-MRI, thereby improving measurements of myocardial perfusion. Also, we have demonstrated that the model can facilitate image reconstruction from sparsely sampled data.

The proposed fixed-point optimization algorithm fails to directly couple the model parameters to the sampled k-space data, thus requiring two cost functions to be minimize. We are currently working on deriving a single cost function that couples the model parameters and k-space data. Further validation of the method in in vivo data is required to evaluate its performance in full detail.



**Figure 2** - Example of respiratory motion correction (a-b) and image reconstruction from sparsely sampled data (e-f) using the proposed unifying model of perfusion and motion. The input images before respiratory motion correction are shown in Figure 1(c-d). The standard projection reconstruction (PR) shown in (c) and (d) demonstrates streaking artifacts due to signal aliasing. These artifacts are removed using the proposed method, while maintaining good resemblance with the true data shown in Figure 1. In both cases, the PR was performed with a sampling percentage of 12.5%, equivalent to 8x data reduction.

#### 5. REFERENCES

- [1] M. Jerosch-Herold, R. T. Seethamraju, C. M. Swingen, N. M. Wilke, and A. E. Stillman, "Analysis of myocardial perfusion MRI," *J. Magn Reson. Imaging*, vol. 19, no. 6, pp. 758-770, June 2004.
- [2] H. B. Larsson, T. Fritz-Hansen, E. Rostrup, L. Sondergaard, P. Ring, and O. Henriksen, "Myocardial perfusion modeling using MRI," *Magn Reson. Med.*, vol. 35, no. 5, pp. 716-726, May 1996.
- [3] J. Tsao, P. Boesiger, and K. P. Pruessmann, "k-t BLAST and k-t SENSE: dynamic MRI with high frame rate exploiting spatiotemporal correlations," *Magn Reson. Med.*, vol. 50, no. 5, pp. 1031-1042, Nov. 2003.
- [4] H. Pedersen, S. Kelle, S. Ringgaard, B. Schnackenburg, E. Nagel, K. Nehrke, and W. Y. Kim, "Quantification of myocardial perfusion using free-breathing MRI and prospective slice tracking," *Magn Reson Med.*, vol. 61, no. 3, pp. 734-738, Mar. 2009.
- [5] S. P. Awate, E. R. Dibella, T. Tasdizen, and R. T. Whitaker, "Model-based image reconstruction for dynamic cardiac perfusion MRI from sparse data," *Conf. Proc. IEEE Eng Med. Biol. Soc.*, vol. 1, pp. 936-941, 2006.